https://doi.org/10.3311/PPci.22101

Periodica Polytechnica Civil Engineering, 68(1), pp. 57–67, 2024

Influence of Climate Change on Probability of Carbonation-Induced Corrosion Initiation

Mostafa Hassan[1], Lamya Amleh[1*]

[1] Department of Civil Engineering, Faculty of Engineering and Architectural Science, Toronto Metropolitan University, 350 Victoria Street, Toronto, ON, M5B 2K3, Canada
[*] Corresponding author, e-mail: lamleh@torontomu.ca

Received: 24 February 2023, Accepted: 18 July 2023, Published online: 23 August 2023

Abstract

The consequences of climate change on infrastructure, particularly reinforced concrete (RC) bridges, have rapidly increased in recent years. These consequences are primarily driven by the surge in CO_2 emissions, which significantly impacts the carbonation depth of RC structures. This study aims to investigate the probability of carbonation-induced corrosion initiation (PCICI) in RC bridge elements. To achieve this, the investigation incorporates a range of concrete covers, varying from 30 to 50 mm, and considers different concrete mixes with cement contents of 400, 350, and 250 kg/m^3. The investigation utilizes the Monte-Carlo simulation method, considering different representative concentration pathways (RCPs) to account for two emission scenarios: RCP2.6 (low emission scenario) and RCP8.5 (high emission scenario). By analyzing projected CO_2 concentrations and maximum temperature, the study provides insights into the potential corrosion initiation risks in RC bridges. The findings indicated a significant 66.3% increase in PCICI for a cement content of 250 kg/m^3, compared to 400 kg/m^3, under the RCP8.5 scenario, specifically when using a concrete cover of 30 mm by 2100. The study also revealed that the PCICI approached an approximate value of zero when concrete covers were set at 45 and 50 mm regardless of the variations in cement contents and the duration considered, for both the RCP2.6 and RCP8.5 scenarios.

Keywords

representative concentration pathways (RCPs), cement contents, concrete covers, Monte Carlo simulation method, carbonation-induced corrosion initiation

1 Introduction

Greenhouse gases, particularly CO_2 emissions, stand as the primary driver of global warming, as extensively documented [1]. The rise in atmospheric CO_2 concentration plays a pivotal role in the escalating global warming phenomenon, leading to adverse consequences such as temperature escalation and sea level rise, and a reduction in relative humidity. Consequently, escalating levels of CO_2 concentration and temperature have far-reaching implications for the durability of reinforced concrete (RC) structures. Carbonation of the concrete cover represents a paramount durability concern for concrete structures, particularly in metropolitan environments. The carbonation process plays a pivotal role in the corrosion of steel reinforcement, making it imperative to address and manage this issue effectively. Carbonation for concrete cover is considered one of the most crucial durability issues for concrete structures in metropolitan environments. The carbonation of concrete is one of the main reasons for the corrosion of steel reinforcement. The microstructure of concrete consists of capillary pores; the amount and type of pores depend on the concrete's quality and the presence of water when mixing concrete [2]. The main factors affecting concrete carbonation are the type and the content of the cement, the water/cement ratio, the degree of hydration, the concentration of CO_2, and the relative humidity [3]. The carbonation mechanism for concrete is an integration of physical and chemical processes [4–6]. Carbonation is a process by which carbonic acid (H_2CO_3), and calcium ion (Ca^{2+}) react from the dissolution of hydrated cement products such as calcium hydroxyl $Ca(OH)_2$, calcium silicate hydrates (C-S-H), and calcium aluminates hydrates (C-A-H) [7, 8]. The reactions lead to the formation of calcium carbonate ($CaCO_3$) which decreases the alkalinity (pH) value of the hardened concrete [9] and results in a small shrinkage for RC members subjected directly to CO_2 emission scenarios [10–13]. The pH value of hardened concrete is generally

Cite this article as: Hassan, M., Amleh, L. "Influence of Climate Change on Probability of Carbonation-Induced Corrosion Initiation", Periodica Polytechnica Civil Engineering, 68(1), pp. 57–67, 2024. https://doi.org/10.3311/PPci.22101

between 12.5 and 13.5, depending on the alkali content of the cement. However, as the concentration of atmospheric CO_2 increases, the pH value of the concrete is reduced to approximately 9.0 [12, 14–16]. Consequently, the protective layer around the reinforcing steel is damaged and the steel is exposed to corrosion [17, 18]. The deterioration of concrete structures is further accelerated by climate change, due to the changing levels of CO_2 concentration, temperature, and relative humidity [19].

Al-Ameeri et al. [20] developed an integrated carbonation model to predict the depth of carbonation in concrete in different climates based on the properties of concrete, concentrations of CO_2, temperature, and humidity. The model was verified by experimental results and found that the worst-case scenario of RCP8.5 could have a significant impact on the durability of concrete structures in the long term. Climate change mitigation measures should be considered to avoid expensive repair and maintenance costs in the future. Great efforts have been made in recent years to reduce the CO_2 concentration in the atmosphere, and one of the most efficient proposed solutions is geological storage. However, progress in geological storage is still slow due to gaps in existing monitoring methods such as seismic methods where full waveform inversion [21] and seismic wave attenuation [22] are proposed as potential methods, but they work with several assumptions. Mizzi et al. [23] investigated how future climate change will affect concrete structures in Malta through carbonation-induced corrosion. Thirteen structures were analyzed retrospectively to validate two carbonation depth prediction models, and these models were used to evaluate the effects of various climate change scenarios on the concrete carbonation depth. It was found that, under the worst-case scenario, there could be an increase in carbonation depth of up to 40% by 2070, reducing the service life of concrete structures.

Carbon dioxide concentrations for four different RCPs are based on simulations from five different earth system models [24]. In this article, the climate scenarios used to project the probability of carbonation-induced corrosion initiation (PCICI) in the future are RCP2.6 and RCP8.5, which are considered the lowest and highest emission scenarios among the different RCPs. RCP8.5 is the worst emission scenario chosen for the concentration of CO_2 [25–27] as shown in Fig. 1.

Carbonation depth depends on many parameters such as concrete quality, concrete cover, relative humidity, and ambient CO_2 concentration. The impact of carbonation

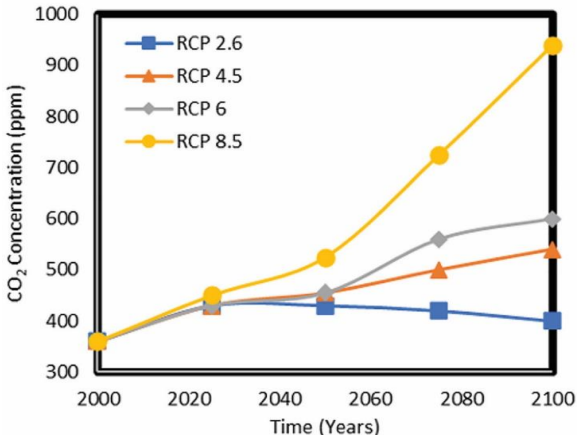

Fig. 1 Projection of atmospheric CO_2 for different emission scenarios [24]

on the environment has been studied by several researchers [28–30]. The influence of the urban environment on atmospheric CO_2 concentrations should be considered for most infrastructure in urban environments. George et al. [31] found that CO_2 concentrations in an urban site were on average 16% higher than those in a rural site. Atmospheric CO_2 concentrations in urban environments would be increased by the (kurban) factor. Similar to Stewart et al. [29], in this research article, the kurban factor is assumed to be normally distributed with a mean of 1.15 and a coefficient of variation of 0.10.

Stewart et al. [29] examined the effects of climate change on corrosion risks for existing concrete infrastructure in Australia. It was found that carbonation-induced damage risks can increase by over 400% by 2100 in inland arid or temperate climates. Risks of chloride-induced corrosion increased by no more than 15%, while corrosion loss of reinforcement amounted to no more than 9.5%. The results were most sensitive to increases in atmospheric CO_2. Structures located in inland arid or temperate climates may require adaptation measures to mitigate damage.

Moreover, Stewart and Peng [32] outlined a method based on reliability to forecast the likelihood of corrosion beginning and causing severe cracking, as well as the recommended increase in design cover needed to offset the increased CO_2 levels and temperatures. A life-cycle costs analysis was conducted to compare the costs of building with the existing covers and the costs of raising design covers, as well as repair and maintenance costs, over the course of a century under the various IPCC carbon dioxide emission scenarios. It was concluded that although the heightened environment of greenhouses will lead to more corrosion in reinforced concrete structures, it may not be worth increasing the concrete covers in terms of the overall cost.

This paper aims to examine the potential effects of climate change on the probability of carbonation-induced corrosion initiation to enhance our understanding of this critical issue. To achieve this objective, the study uses the Monte Carlo simulation method (MCS) to project the PCICI over time, considering various influential factors such as different concrete covers, cement contents, emission scenarios for CO_2, and maximum temperatures in Toronto. Additionally, the article will assess the effect of varying concrete covers (30 to 50 mm) on the PCICI for different emission scenarios and cement contents. By systematically analyzing the impact of these variables, the study strives to provide valuable insights into the complex relationship between climate change and PCICI. Finally, the study will evaluate the difference in the PCICI between the highest emission scenario (RCP8.5) and the lowest emission scenario (RCP2.6) across different years, considering various concrete covers and cement contents. This comparison will offer a comprehensive understanding of the potential consequences of divergent emission scenarios on carbonation-induced corrosion initiation and emphasize the importance of adopting sustainable practices to mitigate climate change effects on infrastructure durability.

The significance of this study lies in the integration of the reliable Monte Carlo simulation method, the consideration of multiple influencing factors, the assessment of varying concrete covers, and the comparison of emission scenarios to comprehensively analyze the potential effects of climate change on the probability of carbonation-induced corrosion initiation. By addressing these aspects, the paper significantly advances the understanding of the complex relationship between climate change and the durability of concrete structures, providing practical insights for designing resilient infrastructure in a changing climate. These findings emphasize the need for implementing effective strategies to mitigate the associated risks, ensuring RC bridge structures' long-term durability and functionality in the face of climate change challenges.

2 Research methodology

The carbonation depth models recommended by Yoon et al. [28], and others consider a wide range of influencing parameters. Moreover, it is predicted as a diffusion process. The carbonation depth over time is calculated using Eq. (1). Moreover, the diffusion coefficient over time is investigated using Eq. (2). Parameter (a) which considers the effect of cement content, and the degree of hydration is calculated using Eq. (3).

$$X_c(t) = \sqrt{2D_{CO_2}(t) \times a^{-1} \times K_{urban} \times C_{CO_2} \times (t-1999)} \times (t_o / (t-1999))^{n_m}, \; t \geq 200, \tag{1}$$

$$D_{CO_2}(t) = D_1 \times (t-1999)^{-n_d}, \tag{2}$$

$$a = 0.75 \times C_e \times C_a o \times \alpha_h \times \left(M_{CO_2} / M_{CaO}\right), \tag{3}$$

where (t) is defined in years starting from the year 2000; $C_{CO_2}(t)$ is the time-dependent mass concentration of CO_2 (1 ppm = 0.0019 × 10^{-3} kg/m^3); K_{urban} is a factor that accounts for increased CO_2 levels in urban environments; $D_{CO_2}(t)$ is the CO_2 diffusion coefficient in concrete; D_1 is the CO_2 diffusion coefficient after one year; n_d is the age factor for the CO_2 diffusion coefficient; t_o is one year; C_e is the cement content (kg/m^3); CaO is the calcium oxide content in cement (0.65); α_H is the degree of hydration; M_{CaO} is the molar mass of the calcium oxide (56 g/mol), and M_{CO_2} is the molar mass of CO_2 (44 g/mol). The age factor for microclimatic conditions (n_m) is equal to 0 for sheltered outdoors, and n_m is equal to 0.12 for unsheltered outdoors. This research study considered the microclimatic conditions as sheltered outdoors, thus (n_m = 0).

The mean values for the diffusion coefficients (D_1) and age factor (n_d) are shown in Table 1 [33, 34]. These parameters are based on temperature (T = 20°C) and relative humidity (RH = 65%).

The degree of hydration for ordinary Portland cement after more than 400 days is calculated through Eq. (4) according to de Larrard [34].

$$\alpha_H \approx 1 - e^{-3.38W/C} \tag{4}$$

The higher temperature will cause an increase in the diffusion coefficient leading to increased carbonation depths [6, 35]. The effect of temperature on the diffusion coefficient is modeled using the Arrhenius law [6, 35, 36]. Precisely, the factor of the temperature used is calculated using Eq. (5). However, the impact of the cracks generated in the concrete on the diffusion coefficient is neglected in this research for conducting the PCICI. The projected annual mean maximum temperature values used in this research are considered for Toronto City at different RCPs as shown in Fig. 2. The two RCPs used in the projection

Table 1 Mean parameter values for the diffusion coefficient and age factor [33, 34]

W/C	$D_1 \times 10^{-4}$ (cm^2/s)	n_d
0.45	0.65	0.218
0.55	2.22	0.240

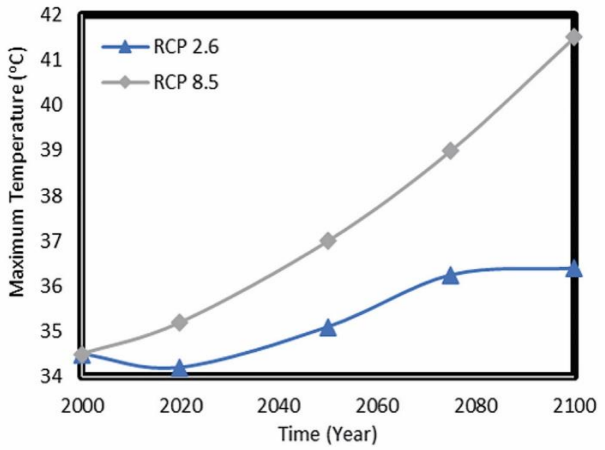

Fig. 2 Projection of annual maximum temperature for Toronto City at different RCPs [37]

for the annual mean maximum temperature are RCP2.6 and RCP8.5. Canada's Changing Climate Report (CCCR) conducted the projection for the annual mean maximum temperature [37].

$$F_T(t) = e^{\frac{E}{R}\times\left(\frac{1}{293}-\frac{1}{273+Tav(t)}\right)} \text{ and}$$
$$T_{av}(t) = \sum_{i=2000}^{t}(T(t)(t-1999)^{-1}) \quad (5)$$

where: $T(t)$ is the temperature (°C) at a time (t), E is the activation energy of the diffusion process (40 kJ/mol), and R is the gas constant (8.314×10^{-3} kJ/mol K).

The carbonation depth at a time (t) assumes that $CO_2(t)$ is constant for all times up to time (t) using Yoon's equation which is given by Eq. (1); that is, a point-in-time predictive model. Additionally, it will result in an overestimate of the carbonation depth as the CO_2 concentration will gradually increase with time up to the peak value of $CO_2(t)$. Stewart et al. [38] considered this phenomenon and calculated carbonation depths due to enhanced atmospheric CO_2 concentrations using the average CO_2 concentration over time. Moreover, Eq. (1) can be rewritten as in Eq. (6).

$$X_c(t) = \sqrt{2 f_T(t)\times D_{co2}(t)\times(1/\mathrm{a})\times K_{urban}\times\int_{2000}^{t} C_{co2}(t)\,dt}$$
$$\times(1/(t-1999))^{n_m},\ t \geq 2000 \quad (6)$$

This research uses the MCS as a computational method to develop a stochastic model for time-dependent reliability analysis. This method is chosen due to its accuracy and suitability for long-term predictions. By increasing the number of samples in the MCS, the accuracy of forecasts improves, allowing for more precise predictions of the probability of corrosion initiation over extended periods. This aligns with the nature of the carbonation-induced corrosion initiation model, where long-term predictions are crucial. For each interval of time, the time-varying probability of carbonation-induced corrosion initiation is predicted in this research using the MCS with 100,000 samples, assuming the random variables follow a normal distribution. Furthermore, in this study, all parameters are assumed to be independent and follow normal distribution functions.

Additionally, reliability serves as a vital indicator of the quality of specialized structures, such as RC bridges, that are exposed to extreme environmental conditions represented by different CO_2 emission scenarios. Reliability is defined as the probability of a performance function, denoted as $g(x)$, exceeding zero ($P\{g(x) > 0\}$). Conversely, the probability of failure is defined as $P\{(g(x) < 0)\}$. Typically, the complement of the probability of failure is calculated to determine reliability. This measure of reliability plays a critical role in assessing the performance and durability of structures subjected to challenging environmental conditions, ensuring their ability to meet specified standards and requirements.

The MCS method is a powerful numerical technique for accurately estimating the probability of carbonation or chloride-induced corrosion initiation [29, 30, 39]. The modeling was performed in this research using MATLAB. Additionally, the MCS method requires the generation of many random numbers [40] and involves three basic steps: (1) selecting the appropriate distribution type for each random variable; (2) generating random numbers based on the selected distribution; and (3) conducting simulations based on the generated random numbers [41]. The limit state function (LSF) is then evaluated for the generated random numbers, where each random number corresponds to a value of the LSF. Finally, an estimation of the probability of corrosion is obtained by counting the number of LSF values less than zero and dividing the count by the total number of data points.

The performance function is generated, as the difference between a term equivalent to resistance and another term equivalent to the load effect. The term resistance is used to refer to the concrete cover that resists corrosion-induced cracking. The term load effect is represented by the carbonation depth calculated over time or the corrosion-induced stresses that lead to cracking. The value of the parameters for the carbonation depth ($X_c(t)$) are functions of several variables such as (Age factor (n_d), Diffusion coefficient (D_1), and K_{urban}). Therefore, the performance

function for corrosion initiation due to CO_2 is formulated as shown in Eq. (7). Corrosion initiation is generated when the carbonation depth exceeds the concrete cover thickness as illustrated in Eq. (7).

$$g(CV, D_1, K_{urban}, n_d) = CV - X_c(t)(D_1, K_{urban}, n_d), \quad (7)$$

where:
$g(CV, D_1, K_{urban}, n_d) = 0$ (limit state),
$g(CV, D_1, K_{urban}, n_d) > 0$ (un-corroded state),
$g(CV, D_1, K_{urban}, n_d) < 0$ (corrosion state).

The MCS method is used to estimate the probability of carbonation-induced corrosion. The LSF is calculated as shown in Eq. (8).

$$LSF = CV - \sqrt{2 f_T(t) \times D_{co2}(t) \times (1/\mathrm{a}) \times K_{urban} \times \int_{2000}^{t} C_{co2}(t)\, dt} \quad (8)$$

where: (CV, D_1, n_d, and K_{urban}) are random variables following normal distribution function.

Generally, corrosion occurs when the carbonation depth reaches the surface of the reinforcing bar. The cumulative probability of corrosion initiation at a time (t) is expressed as in Eq. (9).

$$P_i(t) = \Pr[CV - X_c(t) < 0], \quad (9)$$

where: $X_c(t)$ is the carbonation depth obtained from equation (6), and $P_i(t)$ is the probability of carbonation-induced corrosion initiation over time.

Furthermore, the parameters for the carbonation depth equation (CO_2 is dependent on time) follow a normal distribution function as shown in Table 2. The water-to-cement ratio used in the concrete mixes is equal to 0.45. The mean and the standard deviation for each random variable depend on Stewart et al. [29] assumptions as illustrated in Table 2 for the carbonation-induced corrosion initiation model [42].

The probability of failure in the n-dimensional condition is based on the reliability theory and it can be written using multi-integration on joint probability density function as in Eq. (10) [41, 43].

$$P_f = P[G(\boldsymbol{x}) \le 0] = \int_{G(\boldsymbol{x})\le 0} f(\boldsymbol{x})\, dx, \quad (10)$$

where: $\boldsymbol{x}$ is the random vector which represents random variables and $f(x)$ is the joint probability density function of variables. The reliability index (β) is defined as the shortest distance between the space center of the problem and the limit state function in standard normal coordinates according to Hasofer and Lind [43].

Table 2 Mean, and standard deviation, for random variables related to the carbonation deterioration model

Random variables	CV (mm)	D_1 (mm^2/s)	n_d	K_{urban}
μ	CV + 6 mm	0.65×10^{-2}	0.218	1.15
σ	11.5 mm [42]	0.15×10^{-2}	0.02616	0.115

where: μ is the mean, and σ is the standard deviation for each random variable.

In simple terms, when all the variables follow the normal distribution and are independent of each other, the failure probability is calculated as in Eq. (11).

$$P_f = \varphi(-\beta), \quad (11)$$

where: $\varphi(\beta)$ is the cumulative distribution function and β is the reliability index.

3 Analysis of results

3.1 Prediction of the PCICI for concrete including different concrete covers and cement contents

Stewart and Peng [32] investigated the probability of corrosion initiation in an RC structure with a 30 mm concrete cover, assuming the structure was sheltered outdoors to mitigate environmental exposure. Their study revealed that the probabilities of corrosion initiation considering a water-to-cement ratio of 0.45 and a 30 mm cover, reached values of 0.016 and 0.038 in the year 2100, for the low-emission scenario (B1) and the high-emission scenario (A1F1), respectively. In the current study, the MCS method uses a robust sample size of 100,000 to assess the probabilities of corrosion initiation for the same performance function associated with carbonation-induced corrosion initiation. Our findings verified those of Stewart and Peng [32], with corrosion initiation probabilities of 0.015 and 0.031 for the low and high-emission scenarios, respectively, in 2100, using concrete with a water-to-cement ratio of 0.45 and a 30 mm concrete cover. These results, as depicted in Fig. 3, reaffirm the consistency and agreement between our study and the previous findings by Stewart and Peng [32].

In addition, the probabilities of corrosion initiations were conducted in this research using the MCS consisting of (100,000) samples for the same performance function related to the carbonation-induced corrosion initiation. Finally, it was verified that the probabilities of corrosion initiations reached values of 0.015 and 0.031 which are almost as same as the values obtained by Stewart and Peng [32], for concrete with a water-to-cement ratio of 0.45 and a concrete cover of 30 mm in 2100, for the low and high-emission scenarios, respectively as clarified in Fig. 3.

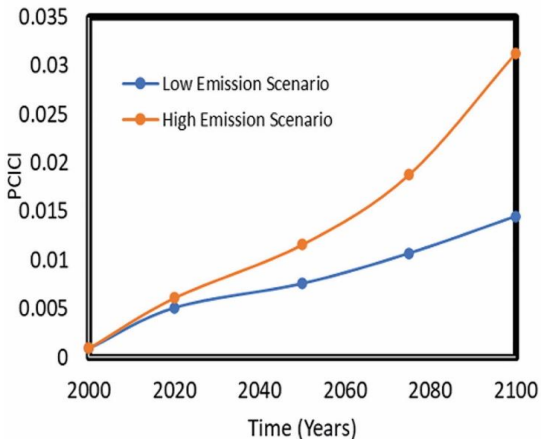

Fig. 3 Probabilities of carbonation-induced corrosion initiations at different emission scenarios

A parametric study was performed using an MCS method consisting of 100,000 samples for each random variable defined in the model to determine the PCICI for different cement contents and RCPs. The CVs used in this study ranged from 30 to 50 mm, with a W/C of 0.45 for both RCP2.6 and RCP8.5, as shown in Fig. 3. For a CV of 30 mm and cement contents of 250 kg/m^3 and 400 kg/m^3, the corresponding PCICI values for RCP2.6 and RCP8.5 in the year 2100 were found to be 0.71×10^{-2} and 0.49×10^{-2}, and 1.43×10^{-2} and 0.86×10^{-2}, respectively, as illustrated in Fig. 4(a) and (b). Moreover, when the CV was increased to 35 mm, the PCICI values for RCP2.6 and RCP8.5 in 2100 were determined to be equal to 2.1×10^{-3} and 1.3×10^{-3} and 4.6×10^{-3} and 2.4×10^{-3} for cement contents of 250 kg/m^3

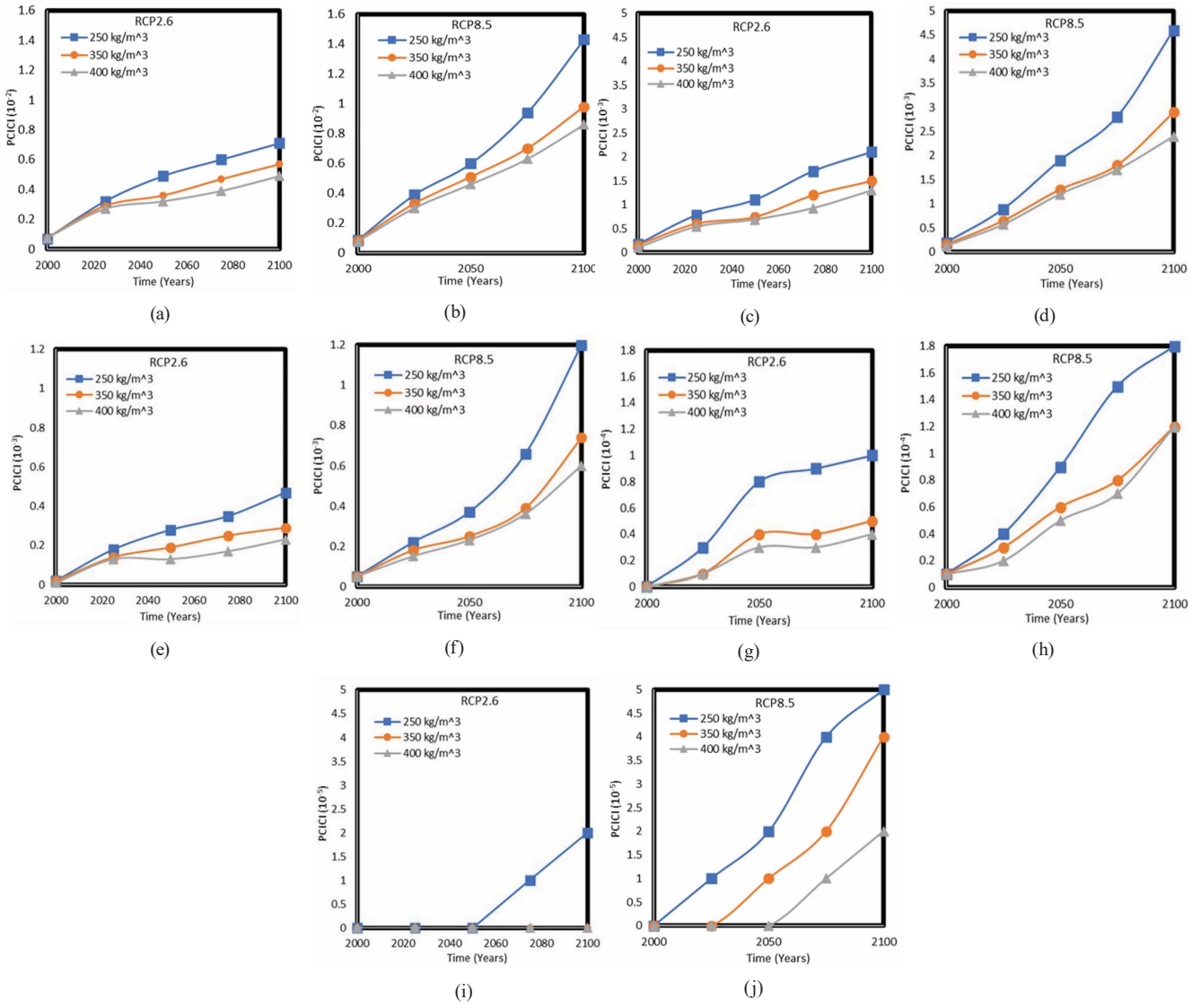

Fig. 4 Probabilities of carbonation-induced corrosion initiations for concrete including different concrete covers, and cement contents at different RCPs; (a) CV = 30 mm, (b) CV = 30 mm, (c) CV = 35 mm, (d) CV = 35 mm, (e) CV = 40 mm, (f) CV = 40 mm, (g) CV = 45 mm, (h) CV = 45 mm, (i) CV = 50 mm, (j) CV = 50 mm

and 400 kg/m^3, respectively, in 2100, as shown in Fig. 4(c) and (d). Finally, for the CV of 40 mm and cement contents of 250 kg/m^3 and 400 kg/m^3, the PCICI values for RCP2.6 and RCP8.5 in 2100 were calculated to be 0.47×10^{-3} and 0.23×10^{-3} and 1.2×10^{-3} and 0.6×10^{-3}, respectively, as illustrated in Fig. 4(e) and (f).

The PCICIs for cement contents equal to 250 kg/m^3 and 400 kg/m^3, respectively, were found to be 1.0×10^{-4} and 0.4×10^{-4}, for RCP2.6 and CV of 45 mm in 2100, when the CV is equal to 45 mm as shown in Fig. 4(g). Similarly, for RCP8.5 when using a 45 mm concrete cover, the PCICI would be 1.8×10^{-4} and 1.2×10^{-4} for cement contents equal to 250 kg/m^3, and 400 kg/m^3, respectively, in 2100, for RCP8.5, as shown in Fig. 4(h). Furthermore, the PCICI would be 2.0×10^{-5} and 0 for 250 kg/m^3 and 400 kg/m^3 cement contents to 250 kg/m^3 and 400 kg/m^3, respectively, in 2100 when the CV is equal to 50 mm for RCP2.6, as indicated in Fig. 4(i). In addition, when the CV is equal to 50 mm, the PCICI would be 5.0×10^{-5} and 2×10^{-5} with 250 kg/m^3 and 400 kg/m^3 cement contents, for RCP8.5, respectively, in 2100, as shown in Fig. 4(j).

The results show that the PCICI values for cement contents equal to 350 and 250 kg/m^3, respectively for both RCP2.6 and RCP8.5, in 2100, changed significantly when the CV reduced from 50 to 30 mm. For RCP2.6, the PCICI changed from (0 and 2.0×10^{-5}) to (0.57×10^{-2} and 0.71×10^{-2}). Similarly, for RCP8.5, the PCICI altered from (4.0×10^{-5} and 5.0×10^{-5}) to (0.98×10^{-2} and 1.43×10^{-2}). Additionally, the PCICI for cement content equal to 250 kg/m^3, when the CV is equal to 30 mm, in 2100, increased drastically by 45% for RCP2.6 and 66% for RCP8.5, in comparison to 400 kg/m^3.

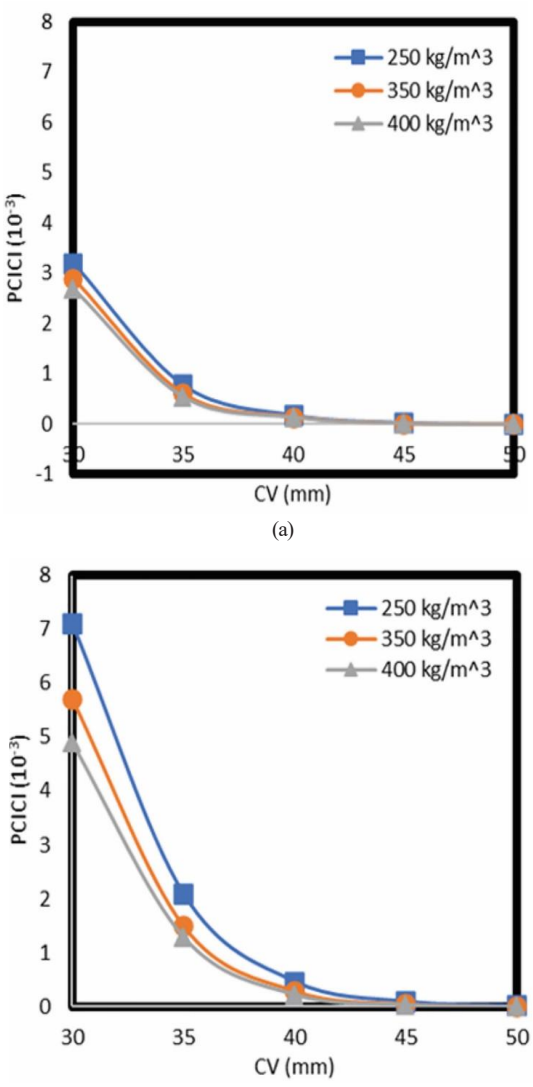

Fig. 5 Probabilities of corrosion initiations versus different (CVs) for different cement contents in different years for RCP2.6; (a) Year 2025, (b) Year 2100

3.2 Effect of different concrete covers and cement contents on the PCICI for different emission scenarios

The PCICI for a cement content of 250 kg/m^3 increased significantly when compared to 400 kg/m^3 for both 2025 and 2100 under the RCP2.6 scenario. In particular, the PCICI increased by 19% when the CV was 30 mm in 2025, as shown in Fig. 5(a). In 2100, the PCICI increased by a staggering 45% when the CV was 30 mm, as shown in Fig. 5(b). It was observed that the PCICI remained almost constant, approximately equal to zero when using 45- and 50-mm CVs as illustrated in Fig. 5, regardless of the cement content or the year, for the RCP2.6 scenario.

The observed trend in the PCICI values changed significantly with a decrease in the cement contents (i.e., PCICI values for cement content of 400 kg/m^3 are lower than the PCICI values for cement content of 250 kg/m^3) for different concrete mixes in both the years 2025 and 2100. Additionally, the PCICI values increased by 30% with cement content equal to 250 kg/m^3 compared to 400 kg/m^3 for the year 2025 when the CV is equal to 30 mm as shown in Fig. 6(a) for RCP8.5. Similarly, the PCICI values increased by 66.3% with cement content equal to 250 kg/m^3 compared to 400 kg/m^3 for the year 2100 when the CV is equal to 30 mm as shown in Fig. 6(b) for RCP8.5. Furthermore, it was found that the PCICI values remain almost constant (approximately equal to zero) for concrete covers of 45 and 50 mm, including different cement contents for both the years 2025 and 2100, as observed in Fig. 6 for RCP8.5.

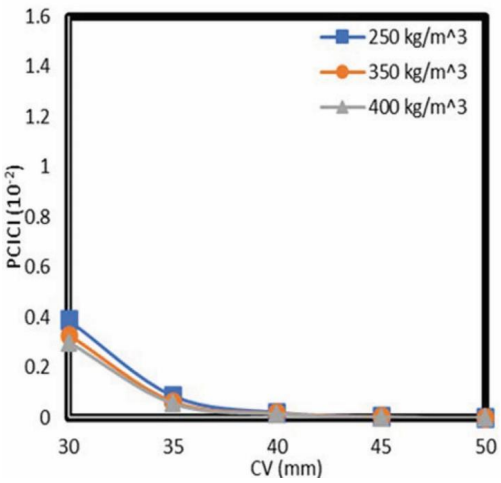

(a)

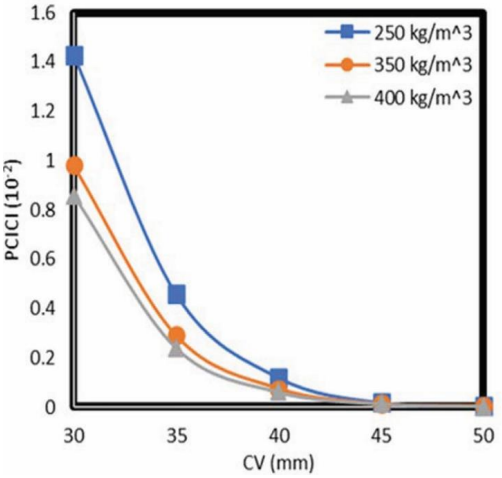

(b)

Fig. 6 Probabilities of corrosion versus different CVs for different cement contents in different years for RCP8.5; (a) Year 2025, (b) Year 2100

3.3 Difference (Δ) between the PCICIs of RCP8.5 and RCP2.6 for concrete having different concrete covers, and cement contents in different years

It was noticed that the difference between the PCICIs of RCP8.5 and RCP2.6 significantly decreased when the concrete cover changed from 30 to 50 mm for different cement contents as illustrated in Fig. 7. It was concluded that the difference between the PCICIs of RCP8.5 and RCP2.6 in 2025 decreased sharply from (7×10^{-4}, 4×10^{-4}, and 3×10^{-4}) to zero values for the following cement contents equal to 250 kg/m^3, 350 kg/m^3, and 400 kg/m^3, respectively, when the CV changed from 30 to 50 mm, as shown in Fig. 7(a). Similarly, the difference between the PCICIs of RCP8.5 and RCP2.6 decreased from (7.2×10^{-3}, 4.1×10^{-3}, and 3.7×10^{-3}) to (0.03×10^{-3}, 0.04×10^{-3}, and 0.02×10^{-3}) for the following cement contents equal to 250 kg/m^3, 350 kg/m^3, and 400 kg/m^3, respectively when the CV changed from 30 to 50 mm, in 2100, as illustrated in Fig. 7(b).

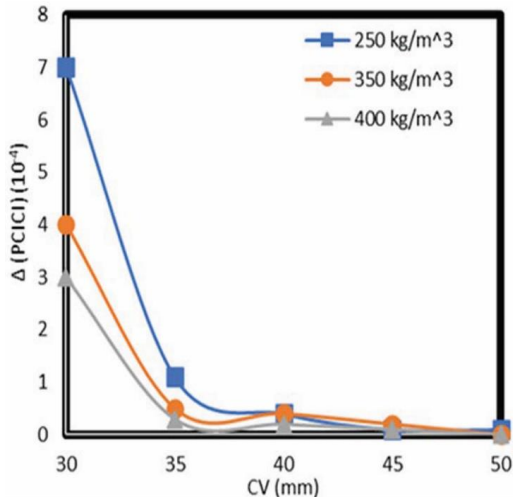

(a)

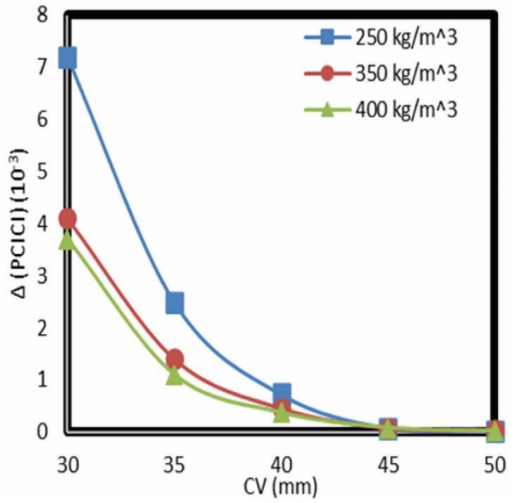

(b)

Fig. 7 Difference in the probabilities of corrosion initiation between RCP8.5 and RCP2.6 for different concrete covers and cement contents in different years; (a) Year 2025, (b) Year 2100

Furthermore, the difference between PCICIs of RCP8.5 and RCP2.6 reached a minimum value when the CVs are equal to 35 mm and 40 mm for different cement contents in 2025, as shown in Fig. 7(a). The difference between the PCICIs reached 2.5×10^{-3} and 0.73×10^{-3}, for CVs equal to 35 mm and 40 mm, respectively, when the cement content equals 250 kg/m^3 in 2100, as shown in Fig. 7(b). Additionally, the difference between the PCICIs of RCP8.5 and RCP2.6 reached 1.1×10^{-3} and 0.37×10^{-3}, when the concrete covers equal to 35 mm and 40 mm, respectively, for cement content of 400 kg/m^3 in 2100, as shown in Fig. 7(b). Finally, it was deduced that the difference between the PCICIs of RCP8.5 and RCP2.6 attained minimum values (approximately equal to zero) when the CVs are equal to 45 mm and 50 mm including different cement contents at different years as shown in Fig. 7.

4 Conclusions

This research study has furthered the understanding of concrete carbonation as a critical deterioration model that occurs in the elements of the RC bridge and its potential effects on steel reinforcement corrosion. By considering different cement contents, including 400 kg/m^3, 350 kg/m^3, and 250 kg/m^3, as well as a water-to-cement ratio of 0.45 and RCP2.6 (low-emission scenario) and RCP8.5 (high-emission scenario) for the concentration of CO_2 and temperature. The MCS was conducted using 100,000 samples. The results of this study provide a comprehensive overview of the probability of carbonation-induced corrosion initiation in concrete structures.

1. It was deduced that the PCICI for a cement content equal to 250 kg/m^3 compared to the PCICI for a cement content of 400 kg/m^3 increased by 19% and 45%, when the CV is equal to 30 mm for 2025 and 2100, respectively, under the RCP2.6 climate scenario. Furthermore, the probability of corrosion initiations increased dramatically by 30% and 66% when the cement content decreased from 400 kg/m^3 to 250 kg/m^3 with 30 mm concrete cover thickness for the RCP8.5 scenario in 2025 and 2100, respectively. Thus, decreasing the cement contents in the concrete mixes will significantly increase the probability of carbonation-induced corrosion initiation.
2. An analysis of the data collected showed that the corrosion initiations' probabilities were almost constant (approximately equal to zero) when the CVs were set to 45 and 50 mm, regardless of various cement contents and emission scenarios (RCP2.6 and RCP8.5) in 2025 and 2100.
3. The projected difference between the PCICIs of RCP8.5 and RCP2.6 scenarios decreased from 7.2×10^{-3} to 3.7×10^{-3} when the cement contents increased from 250 kg/m^3 to 400 kg/m^3, respectively, for concrete cover equal to 30 mm in 2100.
4. Additionally, the difference between the PCICIs of RCP8.5 and RCP2.6 accomplished minimum values when the concrete cover thicknesses were set at 35 and 40 mm for varying cement contents in 2025. Thus, it was observed that concrete with a CV equal to or greater than 40 mm for the elements of the RC bridge hasn't any effect on the difference between the PCICIs of RCP8.5 and RCP2.6 scenarios for different concrete mixes, including different cement contents in 2025.
5. Moreover, the difference between the PCICIs of RCP8.5 and RCP2.6 was achieved at 2.5×10^{-3} and 0.73×10^{-3} when the concrete cover thicknesses are 35 and 40 mm, respectively, for a cement content equal to 250 kg/m^3 in 2100. However, the difference decreased to 1.1×10^{-3} and $0.37 \times 10^{-3}$when the cement content increased to 400 kg/m^3 for the previously mentioned concrete covers in 2100.
6. Finally, it was deduced that the difference between the PCICIs of RCP8.5 and RCP2.6 have reached minimum values (approximately equal to zero) when the CVs are set to 45 and 50 mm for different cement contents in different years in the future.

Acknowledgment

The authors would like to acknowledge the National Research Council Canada (NRCC) in partnership with Toronto Metropolitan University (Formerly, Ryerson University), which has funded this and related research.

Conflict of Interest

The authors declare no conflict of interest.

Credit authorship contribution statement

Mostafa Hassan: Formal analysis, Methodology, Validation, Writing – original draft. *Lamya Amleh*: Methodology, Supervision, Conceptualization, Funding acquisition, Writing – review & editing.

References

[1] Aminzadegan, S., Shahriari, M., Mehranfar, F., Abramović, B. "Factors affecting the emission of pollutants in different types of transportation: A literature review", Energy Reports, 8, pp. 2508–2529, 2022. https://doi.org/10.1016/j.egyr.2022.01.161

[2] Verbeck, G. J. "STP39460S Carbonation of hydrated Portland cement", ASTM Special Technical Publication, 205, pp. 17–36, 1958. https://doi.org/10.1520/STP39460S

[3] Jiang, L., Lin, B., Cai, Y. "A model for predicting carbonation of high-volume fly ash concrete", Cement and Concrete Research, 30(5), pp. 699–702, 2000. https://doi.org/10.1016/S0008-8846(00)00227-1

[4] Huang, Q., Jiang, Z., Zhang, W., Gu, X., Dou, X. "Numerical analysis of the effect of coarse aggregate distribution on concrete carbonation", Construction and Building Materials, 37, pp. 27–35, 2012. https://doi.org/10.1016/j.conbuildmat.2012.06.074

[5] Al Fuhaid, A. F., Niaz, A. "Carbonation and Corrosion Problems in Reinforced Concrete Structures", Buildings, 12(5), 586, 2022. https://doi.org/10.3390/buildings12050586

[6] Tongaria, K., Mandal, S., Mohan, D. "A Review on Carbonation of Concrete and Its Prediction Modelling", Journal of Environmental Nanotechnology, 7(4), pp. 75–90, 2018. https://doi.org/10.13074/jent.2018.12.184325

[7] Glasser, F. P., Matschei, T. "Interactions between Portland cement and carbon dioxide", presented at the 12th International Congress on the Chemistry of Cement, QC, Canada, Montréal, July 8–13, 2007. [online] Available at: https://iccc-online.org/fileadmin/grup-pen/iccc/proceedings/12/pdf/fin00170.pdf

[8] Park, D. C. "Carbonation of concrete in relation to CO2 permeability and degradation of coatings", Construction, and Building Materials, 22(11), pp. 2260–2268, 2008. https://doi.org/10.1016/j.conbuildmat.2007.07.032

[9] Bouchaala, F., Payan, C., Garnier, V., Balayssac, J. P. "Carbonation assessment in concrete by nonlinear ultrasound", Cement and Concrete Research, 41, pp. 557–559, 2011. https://doi.org/10.1016/j.cemconres.2011.02.006

[10] Chi, J. M., Huang, R., Yang, C. C. "Effects of carbonation on mechanical properties and durability of concrete using the accelerated testing method", Journal of Marine Science and Technology, 10(1), pp. 14–20, 2002. https://doi.org/10.51400/2709-6998.2296

[11] Bier, TH. A., Kropp, J., Hilsdorf, H. K. "Formation of silica gel during carbonation of cementitious systems containing slag cements", ACI Symposium Paper, 114, pp. 1413–1428, 1989. https://doi.org/10.14359/1817

[12] Jedidi, M., Belhassen, A. " Carbonation of Reinforced Concrete Structures", Current Trends in Civil and Structural Engineering, 5(2), 2020. https://doi.org/10.33552/CTCSE.2020.05.000609

[13] Mahmood, W., Khan, A., Ayub, T. "Carbonation Resistance in Ordinary Portland Cement Concrete with and without Recycled Coarse Aggregate in Natural and Simulated Environment", Sustainability, 14(1), 437, 2022. https://doi.org/10.3390/su14010437

[14] Papadakis, V. G., Vayenas, C. G., Fardis, M. G. "Fundamental Modeling and Experimental Investigation of Concrete Carbonation", ACI Materials Journal, 88(4), pp. 363–373, 1991. https://doi.org/10.14359/1863

[15] Bentur, A., Berke, N., Diamond, S. "Steel Corrosion in Concrete", CRC Press, 1997. ISBN: 9781482271898 https://doi.org/10.1201/9781482271898

[16] Gu, H., Li, Q. "Updating deterioration models of reinforced concrete structures in carbonation environment using in-situ inspection data", Structure and Infrastructure Engineering, 18(2), pp. 266–277, 2022. https://doi.org/10.1080/15732479.2020.1841246

[17] Alonso, C., Andrade, C., González, J. A. "Relation between resistivity and corrosion rate of reinforcements in carbonated mortar made with several cement types", Cement and Concrete Research, 18, pp. 687–698, 1988. https://doi.org/10.1016/0008-8846(88)90091-9

[18] Anstice, D. J., Page, C. L., Page, M. M. "The pore solution phase of carbonated cement pastes", Cement and Concrete Research, 35, pp. 377–383, 2005. https://doi.org/10.1016/j.cemconres.2004.06.041

[19] Wang, X., Stewart, M. G., Nguyen, M. "Impact of climate change on corrosion and damage to concrete infrastructure in Australia", Climatic Change, 110, pp. 941–957, 2012. https://doi.org/10.1007/s10584-011-0124-7

[20] Al-Ameeri, A. S., Rafiq, M. I., Tsioulou, O., Rybdylova, O. "Impact of climate change on the carbonation in concrete due to carbon dioxide ingress: Experimental investigation and modeling", Journal of Building Engineering, 44, 102594, 2021. https://doi.org/10.1016/j.jobe.2021.102594

[21] Takam Takougang, E. M., Ali, M. Y., Bouzidi, Y., Bouchaala, F., Sultan, A. A., Mohamed, A. I. "Characterization of a carbonate reservoir using elastic full-waveform inversion of vertical seismic profile data", Geophysical Prospecting, 68(6), pp. 1944–1957, 2020. https://doi.org/10.1111/1365-2478.12962

[22] Bouchaala, F., Ali., M. Y., Matsushima, J. "Attenuation study of a clay-rich dense zone in fractured carbonate reservoirs", Geophysics, 84(3), pp. B205–B216, 2019. https://doi.org/10.1190/geo2018-0419.1

[23] Mizzi, B., Wang, Y., Borg, R. P. "Effects of climate change on structures; analysis of carbonation-induced corrosion in Reinforced Concrete Structures in Malta", IOP Conference Series: Materials Science and Engineering, 442, 012023, 2018. https://doi.org/10.1088/1757-899X/442/1/012023

[24] Core Writing Team, Pachauri, R. K., Meyer L.vv (eds.) "IPCC 2014: Climate Change 2014: Synthesis Report", Contribution of Working Groups I, II and III to the Fifth Assessment Report of the Intergovernmental Panel on Climate Change, IPCC, Geneva, Switzerland, 2015. ISBN: 978-92-9169-143-2 [online] Available at: https://epic.awi.de/id/eprint/37530/1/IPCC_AR5_SYR_Final.pdf

[25] Intergovernmental Panel on Climate Change (IPCC) "Anthropogenic and Natural Radiative Forcing", In: Climate Change 2013 – The Physical Science Basis: Working Group I Contribution to the Fifth Assessment Report of the Intergovernmental Panel on Climate Change, Cambridge University Press, 2014, pp. 659–740. ISBN: 9781107415324 https://doi.org/10.1017/CBO9781107415324.018

[26] Intergovernmental Panel on Climate Change (IPCC) "Long-term Climate Change: Projections, Commitments and Irreversibility Pages 1029 to 1076", In: Climate Change 2013 – The Physical Science Basis: Working Group I Contribution to the Fifth Assessment Report of the Intergovernmental Panel on Climate Change, Cambridge University Press, 2014, pp. 1029–1136. ISBN: 9781107415324. https://doi.org/10.1017/CBO9781107415324.024

[27] van Vuuren, D. P., Edmonds, J., Kainuma, M., Riahi, K., Thomson, A., …, Rose, S. K. "The representative concentration pathways: an overview", Climatic Change, 109, pp. 5–31, 2011. https://doi.org/10.1007/s10584-011-0148-z

[28] Yoon, I.-S., Çopuroğlu, O., Park, K.-B. "Effect of global climatic change on carbonation progress of concrete", Atmospheric Environment, 41, pp. 7274–7285, 2007. https://doi.org/10.1016/j.atmosenv.2007.05.028

[29] Stewart, M. G., Wang, X., Nguyen, M. N. "Climate change impact and risks of concrete infrastructure deterioration", Engineering Structures, 33, pp. 1326–1337, 2011. https://doi.org/10.1016/j.engstruct.2011.01.010

[30] Hassan, M., Amleh, L., Othman, H. "Effect of Different Cement Content and Water Cement Ratio on Carbonation Depth and Probability of Carbonation Induced Corrosion for Concrete", Cement Wapno Beton, 27(2), pp. 126–143, 2022. https://doi.org/10.32047/CWB.2022.27.2.4

[31] George, K., Ziska, L. H., Bunce, J. A., Quebedeaux, B. "Elevated atmospheric CO_2 concentration and temperature across an urban-rural transect", Atmospheric Environment, 41, pp. 7654–7665, 2007. https://doi.org/10.1016/j.atmosenv.2007.08.018

[32] Stewart, M. G., Peng, J. "Life cycle cost assessment of climate change adaptation measures to minimize carbonation-induced corrosion risks", International Journal of Engineering Under Uncertainty: Hazards, Assessment, and Mitigation, 2(1), pp. 35–46, 2010.

[33] Sanjuán, M. A., del Olmo, C. "Carbonation resistance of one industrial mortar used as a concrete coating", Building, and Environment, 36(8), pp. 949–953, 2001. https://doi.org/10.1016/S0360-1323(00)00045-7

[34] de Larrard, F. "Concrete mixtures proportioning", CRC Press, 1999. ISBN: 9780429179099 https://doi.org/10.1201/9781482272055

[35] Baccay, M. A., Otsuki, N., Nishida, T., Maruyama, S. "Influence of cement type and temperature on the steel corrosion rate in concrete exposed to carbonation", Corrosion, 62(6), pp. 811–821, 2006. https://doi.org/10.5006/1.3278306

[36] DuraCrete "Statistical quantification of the variables in the limit state functions", Contract BRPR-CT95-0132. Project BE95-1347/R9, 2000.

[37] Bush, E., Bonsal, B., Derksen, C., Flato, G., Fyfe, J., …., Zhang, X. "Canada's Changing Climate Report in Light of the Latest Global Science Assessment", Government of Canada, 2022. https://doi.org/10.4095/329703

[38] Stewart, M. G., Teply, B., Králová, H. "The effect of temporal and spatial variability of ambient carbon dioxide concentrations on carbonation of RC structures", presented at the 9th international conference on Durability of Materials and Components, CSIRO, Paper 246, Brisbane, Australia, March, 17–20, 2002.

[39] Saassouh, B., Lounis, Z. "Probabilistic modeling of chloride-induced corrosion in concrete structures using first- and second-order reliability methods", Cement and Concrete Composites, 34, pp. 1082–1093, 2012. https://doi.org/10.1016/j.cemconcomp.2012.05.001

[40] Kroese, D. P., Brereton, T., Taimre, T., Botev, Z. I. "Why the Monte Carlo method is so important today", WIREs Computational Statistics, 6(6), pp. 386–392, 2014. https://doi.org/10.1002/wics.1314

[41] Choi, S.-K., Canfield, R. A., Grandhi, R. V. "Estimation of structural reliability for Gaussian random fields", Structure Infrastructure Engineering, 2, pp. 161–173, 2006. https://doi.org/10.1080/15732470600590192

[42] McGee, R. "Modeling of durability performance of Tasmanian Bridges", In: Applications of Statistics and Probability in Civil Engineering, Proceedings of the ICASP8 Conference, Sydney, Australia, 1999, pp. 297–306. ISBN: 9058090868

[43] Hasofer, A. M., Lind, N. C. "Exact and invariant second-moment code format", Journal of the Engineering Mechanics Division, 100(1), pp. 111–121, 1974. https://doi.org/10.1061/JMCEA3.0001848